Impact of hydroxyl group on adsorption behavior and corrosion inhibition of Schiff-base derivative on carbon steel in 1 M HCl

R.K. Ahmed,¹ A. Mohammed,² M.A.I. Al-Hamid,³ A.M. Mustafa,⁴ F.F. Sayyid,⁴ A.H. Kadhum⁵ and A. Alamiery⁶*

¹Department of Petroleum and Gas Refining Engineering, College of Petroleum Processes Engineering, Tikrit University, Saladin 34001, Iraq

²Department of Electromechanical Engineering, University of Technology, P.O. Box: 10001, Baghdad, Iraq

³Energy and Renewable Energies Technology Centre, University of Technology, Baghdad 10001, Iraq

⁴Department of Production Engineering and Metallurgical, University of Technology, Baghdad, 10001, Iraq

⁵Faculty of Medicine, University of Al-Ameed, P.O. Box: 56001, Karbala, Iraq ⁶Al-Ayen Scientific Research Center, Al-Ayen Iraqi University, AUIQ, An Nasiriyah, P.O. Box: 64004, Thi Qar, Iraq

*E-mail: dr.ahmed1975@gmail.com

Abstract

The study explores the impact of the hydroxyl group on the adsorption and the corrosion inhibition characteristics of 2-((thiazol-2-ylimino)methyl)phenol (TMP), a Schiff-base derivative, on carbon steel in 1 M hydrochloric acid (HCl) medium. Using weight loss methods measurable to ASTM standards, and computational DFT techniques, the research reveals significant insights into the electronic properties and adsorption mechanisms of TMP. Based on their results, it was concluded that TMP acts as a corrosion inhibitor and that the presence of OH group increases TMP adsorption which enhances corrosion inhibition. At 0.5 mM concentration of TMP, an inhibition efficiency of 89.7% was achieved after 5 hours of immersion at 303 K. Their observations showed that there is an increase in efficiency with the time of immersion up to 10 hours. However, around 48 hours there was a slight decrease in efficiency. Studies involving temperature showed improvement in inhibition efficiency at elevated temperatures (303-333 K); also observed inhibition efficiency was aligned with the Langmuir adsorption isotherm. DFT analysis supported the experimental results, identifying TMP as an effective inhibitor for carbon steel corrosion in acidic solutions. The research highlighted the importance of functional groups in designing corrosion inhibitors tailored toward industrial needs.

Received: January 1, 2025. Published: June 6, 2025 doi: 10.17675/2305-6894-2025-14-2-22

Keywords: phenol, thiazole, corrosion, DFT, ASTM.

1. Introduction

Corrosion can occur in different settings and it is an ever increasing challenge in terms of its economical and operational factors. The corrosive costing is somewhere between 3-4% to the entire global GDP equaling trillions of dollars. Corrosion leads to the structural impacts which leads to deep damage in equipment ineffective plans must bring put in place [1, 2]. Hydrochloric acid (HCl) is widely used in the industry for pickling, descaling, acid cleaning of steel and other processes. The most serious drawback is the aggressiveness of HCl which increases the rate of corrosion of carbon steel, the most economical and widely used material. To ensure efficiency in processes and minimize damage to equipment, effective mitigation of HCl-induced corrosion is a prerequisite [3, 4]. Corrosion inhibitors are the principal means of protecting metals from acid corrosion, providing a protective film that inhibits the metallic surface from corroding. Among them, Inorganic inhibitors like chromates and phosphates have been used for a long time because they are protective. However, their use is more and more limited because they are too harmful to human health and the environment because most of them are toxic and non-biodegradable [5, 6]. Organic inhibitors are most sought after because they are friendlier to the environment, are biodegradable, and adsorption on the metal surface takes place through heteroatoms (N, O, S) as well as through aromatic rings and π -electrons. These compounds can be considered cost-effective and sustainable alternatives to inorganic inhibitors because they provide great efficiency at low concentrations [7]. There has been great interest toward the use of Schiff bases as effective corrosion inhibitors for carbon steel in acidic medium in recent years. The adsorbate surface interaction along with the electron donating functional groups tend to enhance the desorption occurring on metal atoms. For example, in consideration of compounds 3-((4-hydroxybenzylidene)amino)-2-methylquinazolin-4(3H)-one (BZ3) and 3-((4-dimethylamino)benzylidene)amino)-2-methylquinazolin-4(3H)-one (BZ4) the respective researched inhibition efficiencies have been reported as 92% and 96% [8]. TMP is characterized by lower toxicity, aligning with the growing emphasis on eco-friendly corrosion inhibitors. This attribute enhances its suitability for industrial applications where environmental considerations are paramount [9]. From an economic perspective, TMP's high inhibition efficiency at low concentrations translates to cost-effectiveness. The ability to achieve substantial corrosion protection with minimal inhibitor usage reduces material costs and minimizes the frequency of maintenance interventions, offering economic advantages over less efficient inhibitors [10].

The simplicity and reliability of weight loss techniques, together with their capability to provide absolute metal loss measurements from conditions to conditions, have rendered them a mainstay in the studies of corrosion inhibition [11, 12]. The method does not provide detailed mechanistic information but is regarded as a very important experimental technique when coupled with a theoretical study such as Density Functional Theory (DFT) for complete understating [13, 14]. The application of Schiff-base derivatives as organic inhibitors has been explored in a number of studies. An example of such work is where it

was shown that these compounds are effective in acidic media due to the presence of hydroxyl and imine functional groups that improve adsorption on metal surfaces [15]. DFT studies further corroborate this finding with the connection of molecular properties to inhibition efficiencies [16, 17]. Other works have studied effects including temperature, concentration, and immersion time on inhibition behavior. This defined the efficiency of inhibition normally increases with concentration and temperature to certain limits, thereby satisfying the adsorption isotherms, for example, Langmuir and Freundlich models [19, 20]. Prolong immersion can lead to desorption or depletion of inhibitors and deficiency of efficiency over time. Although many steps have been taken, most of the investigations conducted to date focus on very narrow experimental conditions and mostly ignore the synergistic effects of some specific functional groups on the adsorption behavior. Many studies also have been disappointed with respect to the theoretical and experimental approaches in terms of synergies.

Carbon steel, a key material in industrial processes, remains vulnerable to HCl-induced corrosion, leading to substantial economic and operational challenges. While Schiff-base derivatives have shown promise as organic inhibitors, there is limited understanding of how specific functional groups, such as hydroxyl groups, influence adsorption mechanisms and inhibition performance. Furthermore, comprehensive studies integrating weight loss methods and theoretical insights are scarce. This study investigates the specific impact of the hydroxyl group on the adsorption behavior and corrosion inhibition efficiency of a Schiff-base derivative, TMP (Figure 1), on carbon steel in a 1 M HCl solution. The research uniquely integrates experimental weight loss techniques with theoretical DFT calculations to provide a holistic understanding of the inhibitor's performance. The main objectives of this work can be summaries as follows:

- 1. To evaluate the corrosion inhibition efficiency of TMP on carbon steel in 1 M HCl using weight loss techniques.
- 2. To investigate the influence of functional groups, particularly hydroxyl group, on adsorption behavior and performance.
- 3. To assess the effect of key variables, including inhibitor concentration, immersion time, and temperature, on inhibition efficiency.
- 4. To validate experimental findings with DFT calculations, linking molecular properties to corrosion inhibition performance.
- 5. To establish adsorption behavior through isotherm modeling, providing mechanistic insights into the inhibitor-metal interaction.

Figure 1. The chemical structure of TMP.

2. Experimental Details

2.1. Materials

The material used in this study was carbon steel with the following chemical composition: 0.21 wt% carbon (C), 0.005 wt% manganese (Mn), 0.38 wt% silicon (Si), 0.05 wt% sulfur (S), 0.01 wt% aluminum (Al), and 0.09 wt% phosphorus (P), with the balance being iron (Fe). The corrosion inhibition behavior of 1-((thiazol-2-ylimino)methyl)-2-naphthol (TMP) was assessed in a 1 M hydrochloric acid (HCl) solution. Steel specimens were prepared in dimensions of 4.0 cm×2.5 cm×0.1 cm. The surfaces of the specimens were polished sequentially with abrasive papers of varying grit sizes (400, 600, and 1200) to achieve a smooth finish. Following polishing, the samples were thoroughly washed with double-distilled water, cleaned with ethanol to remove any residual impurities, dried at room temperature, and weighed to record their initial dry weight for subsequent comparisons [21, 22].

2.2. Preparation of hydrochloric acid solutions

A 1 M HCl solution was prepared by diluting analytical-grade hydrochloric acid (37% purity, Merck, Malaysia) with double-distilled water. TMP was dissolved in the solution at varying concentrations and mixed using a magnetic stirrer to achieve uniform dispersion and homogeneity. Steel samples were immersed in these prepared solutions for predefined time intervals to study corrosion behavior. Any visible signs of corrosion, such as discoloration or surface roughening, were noted. Quantitative analysis of corrosion was performed using weight loss measurements [22, 23].

2.3. Weight loss measurements

The weight loss method was employed to evaluate both the corrosion rate and the inhibition efficiency of TMP on carbon steel in a 1 M HCl environment. Each experiment involved immersing a steel sample with a 1 cm² exposed surface area in 500 mL of the acid solution contained within a glass beaker. TMP concentrations ranged from 0.1 mM to 1 mM, and the temperature was controlled between 303 K and 333 K using a thermostat water bath. Immersion durations were set at 5, 10, 24, and 48 hours. After immersion, samples were cleaned using an ultrasonic cleaner with ultrapure water and ethanol, dried, and reweighed to determine weight loss. The weight loss data were subsequently used to compute the corrosion rate, inhibition efficiency, and surface coverage. The experimental setup, as shown in Figure 2, involved suspending the steel specimen in the acid solution using a chemically inert, non-metallic (Teflon-coated) wire to prevent galvanic coupling and ensure no interference with the corrosion process. The study adhered to NACE standards for corrosion experiments to ensure reproducibility and reliability [22, 23].

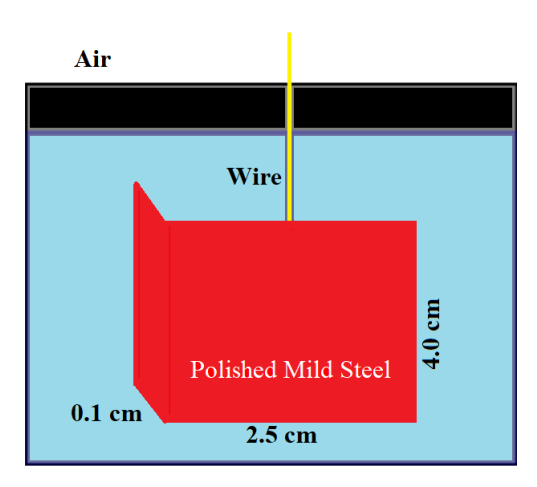


Figure 2. Experimental setup for weight loss corrosion test.

The equations (1-3) were employed for calculations:

$$C_{\rm R} = \frac{W}{at} \tag{1}$$

W is the weight loss (g), a is the exposed surface area of the steel sample (cm 2), and t is the immersion time (hours).

$$IE\% = \left[1 - \frac{C_{R(i)}}{C_{R(0)}}\right] \times 100$$
 (2)

where: $C_{R(0)}$ is the corrosion rate without the inhibitor (control), $C_{R(i)}$ is the corrosion rate with the inhibitor.

$$\theta = 1 - \frac{C_{R(i)}}{C_{R(0)}} \tag{3}$$

To ensure the accuracy and reliability of the experimental data, all weight loss measurements were performed in triplicate under identical conditions. The average values were calculated and reported along with their corresponding standard deviations. This approach minimizes random errors and enhances the reproducibility of the results.

2.4. Theoretical study

Quantum chemical calculations were carried out using GAMESS software to explore the electronic properties of TMP. The molecular structure was optimized using the DFT-B3LYP/6-31G(d) level of theory [24, 25]. The following quantum chemical parameters were calculated regarding equations (4–8):

Ionization potential (I):
$$I = -E_{\text{HOMO}}$$
 (4)

Electron affinity (A):
$$A = -E_{\text{LUMO}}$$
 (5)

Electronegativity (
$$\chi$$
):
$$\chi = \frac{I + A}{2}$$
 (6)

Chemical hardness (
$$\eta$$
):
$$\eta = \frac{I - A}{2}$$
 (7)

Chemical softness (
$$\sigma$$
): $\sigma = \eta^{-1}$ (8)

The electron transfer fraction (ΔN) between the inhibitor and the carbon steel surface was also computed based on equation (9):

$$\Delta N = \frac{7 - \chi_{\text{inh}}}{2\eta_{\text{inh}}} \tag{9}$$

where χ_{inh} and η_{inh} refer to the electronegativity and hardness of the inhibitor, respectively. For these calculations, the reference values for iron (Fe) were taken as $\chi_{Fe}=7~eV$ and $\eta_{Fe}=0~eV$.

These calculations provided insights into the electronic interactions between TMP and the steel surface, elucidating the molecular mechanisms responsible for its corrosion inhibition performance.

3. Results and Discussion

3.1. Weight loss measurements

3.1.1. Effect of immersion time

The weight loss measurements were conducted to evaluate the corrosion rate (C_R) and inhibition efficiency (IE%) of TMP on carbon steel at different inhibitor concentrations and immersion times. The results, summarized in Figure 3, reveal significant trends regarding the impact of immersion time and inhibitor concentration on corrosion behavior. The corrosion rate decreases with increasing TMP concentration for all immersion times, as shown in Figure 3. At 1-hour immersion time, the C_R reduces from 1.21 mg·cm^{-2·h⁻¹} for 0.1 mM TMP to 0.56 mg·cm^{-2·h⁻¹} for 0.5 mM TMP, indicating a clear concentration-dependent inhibition effect. This trend is consistent across other immersion times, with the lowest corrosion rate observed for 0.5 mM TMP at all durations. For extended immersion times (5, 10, 24, and 48 hours), the C_R continues to exhibit a downward trend, though the reduction becomes less pronounced. For example, at 48 hours, the C_R decreases to 0.89 mg·cm^{-2·h⁻¹} for 0.1 mM TMP and 0.34 mg·cm^{-2·h⁻¹} for 0.5 mM TMP. This reduction highlights the sustained adsorption of TMP molecules on the steel surface, forming a protective layer over time. However, a slight increase in C_R is observed after 24 hours for lower TMP concentrations, which may indicate desorption or degradation of the inhibitor.

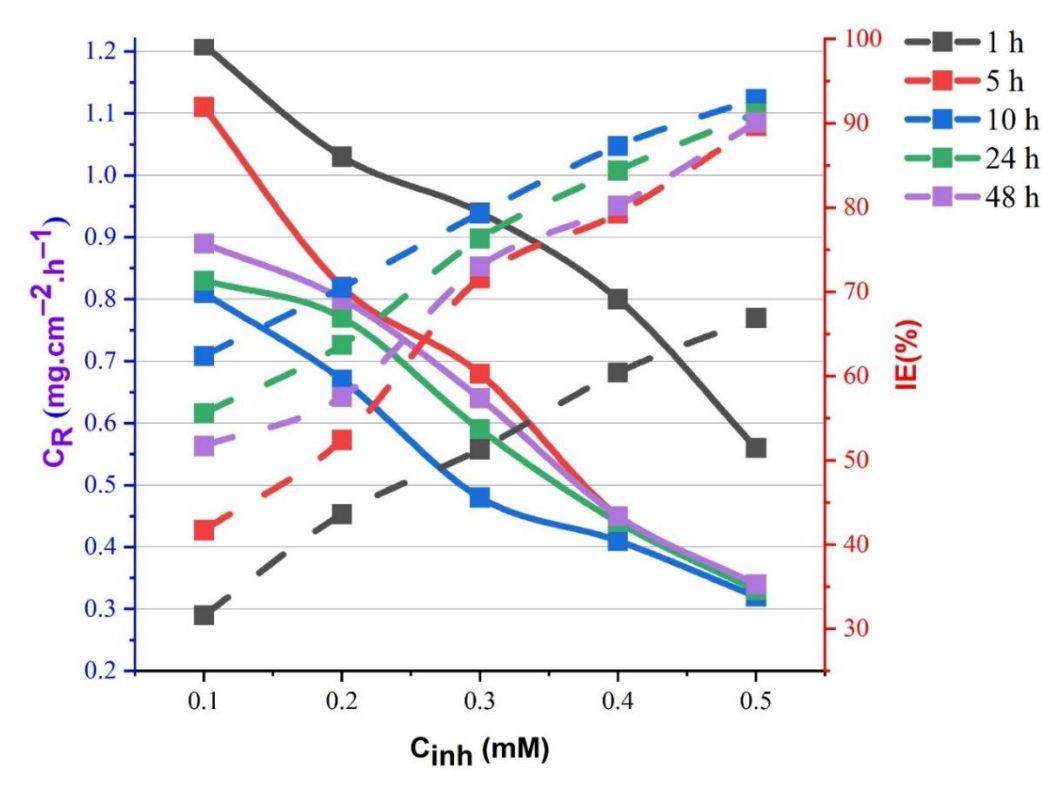


Figure 3. Effect of immersion time and TMP concentration on C_R and inhibition efficiency (IE%) of carbon steel in 1 M HCl solution.

The inhibition efficiency (IE%) shows a consistent increase with higher TMP concentrations, reaching a maximum of 92.9% for 0.5 mM TMP at 10 hours of immersion. At 1 hour, IE% ranges from 31.6% (0.1 mM TMP) to 66.9% (0.5 mM TMP), demonstrating that the initial adsorption of TMP molecules is concentration-dependent. The efficiency continues to improve with longer immersion times, peaking at 10 hours for all concentrations. For instance, IE% at 10 hours is 62.4%, 70.5%, 79.3%, 87.3%, and 92.9% for TMP concentrations of 0.1 mM, 0.2 mM, 0.3 mM, 0.4 mM, and 0.5 mM, respectively. This behavior suggests that prolonged exposure enhances the formation and stabilization of the protective TMP layer. However, beyond 10 hours, IE% begins to decline slightly, particularly for lower TMP concentrations. For example, IE% at 48 hours drops to 51.7% for 0.1 mM TMP and 90.1% for 0.5 mM TMP. This decline could result from the desorption of TMP molecules or the dissolution of the protective film under extended exposure to the acidic medium. The interplay between TMP concentration and immersion time significantly affects the corrosion inhibition performance. High TMP concentrations exhibit better performance over all time intervals, with minimal loss in IE% even at 48 hours. Conversely, at lower concentrations (0.1–0.2 mM), the inhibitor's effectiveness diminishes more rapidly over time, likely due to incomplete surface coverage and lower adsorption strength. At short immersion times (1–5 hours), the inhibition efficiency is primarily governed by the rate of TMP adsorption onto the steel surface. For longer durations (10–48 hours), the stability and durability of the adsorbed TMP film become crucial. TMP demonstrates exceptional stability

at higher concentrations, as evidenced by IE% values above 90% at 48 hours for 0.5 mM TMP. The observed trends in C_R and IE% align with Langmuir adsorption isotherm assumptions, where the inhibitor molecules form a monolayer on the metal surface, and adsorption strength increases with concentration. The ability of TMP to maintain high inhibition efficiency over extended durations highlights its potential as a robust corrosion inhibitor in acidic environments [26]. We have incorporated data from the literature on Schiff-base derivatives without the OH group to serve as a benchmark. For instance, a study on Schiff bases derived from amino acids demonstrated that these compounds exhibit effective corrosion inhibition due to their adsorption capabilities and film-forming properties [9]. However, the absence of the OH group in these derivatives led to a maximum inhibition efficiency lower than for TMP. To this effect, Schiff bases lacking OH moieties achieved around 75%-inhibition efficiency at similar concentration and conditions, while the inhibited TMP with the OH moiety reach as much as 89.7%. This comparison gives an idea about the increasing effect of OH group on the adsorption strength and inhibition efficiency of TMP. We have refined our discussion by explaining that in addition to the hydroxyl moiety, the thiazole ring with nitrogen and sulfur atom in TMP also contributes appreciably to its adsorptive behavior in addition to hydroxyl moiety. The two voids of hetero-atom facilitate the cooperative bonding for coordination with the metal surface, and that ultimately enhances its inhibition performance [27]. Therefore, this will give an insight into the contribution of these functional groups together in the corrosion inhibition character of TMP. It combines this comparative interpretation with an explanation of the role of specific functional groups, through which the study could provide a strong justification for the beneficial action hydroxyl group had on TMP's corrosion inhibition performance.

3.1.2. Effect of temperature

Evaluating the temperature influence on corrosion rates (C_R) and inhibition efficiency (IE%) of TMP in 1 M HCl corroborated between 303 K and 333 K, as illustrated in Figure 4. For C_R values at varying TMP concentrations, increases in concentration at all temperatures were noted-for instance, with rising temperature at 303 K, C_R goes down from 0.81 to 0.32 mg·cm^{-2·h⁻¹} with an increase in TMP concentration from 0.1 to 0.5 mM. The same characteristic was found for the other temperatures, which had the least C_R value at all times in the substrate concentration of 0.5 mM. It was consistent, however, that the C_R further decreased with the increase of temperature at every concentration, implicating much more intensity in adsorption and formation of a more stable protective layer. Also, the IE% improved as in both concentration of TMP and temperature. At 303 K, IE% increased from 41.7% to 89.7% (0.1 to 0.5 mM TMP), while the highest value reached 94.3% at 0.5 mM TMP at the highest temperature of 333 K. Likewise, at 0.4 mM, it improved from 79.3% to 88.4%. The effects of temperature and concentration make a significant contribution to the understanding of the proof that inhibition performance of TMP is increased with temperature owing to a better adsorption onto the surface of steel [28].

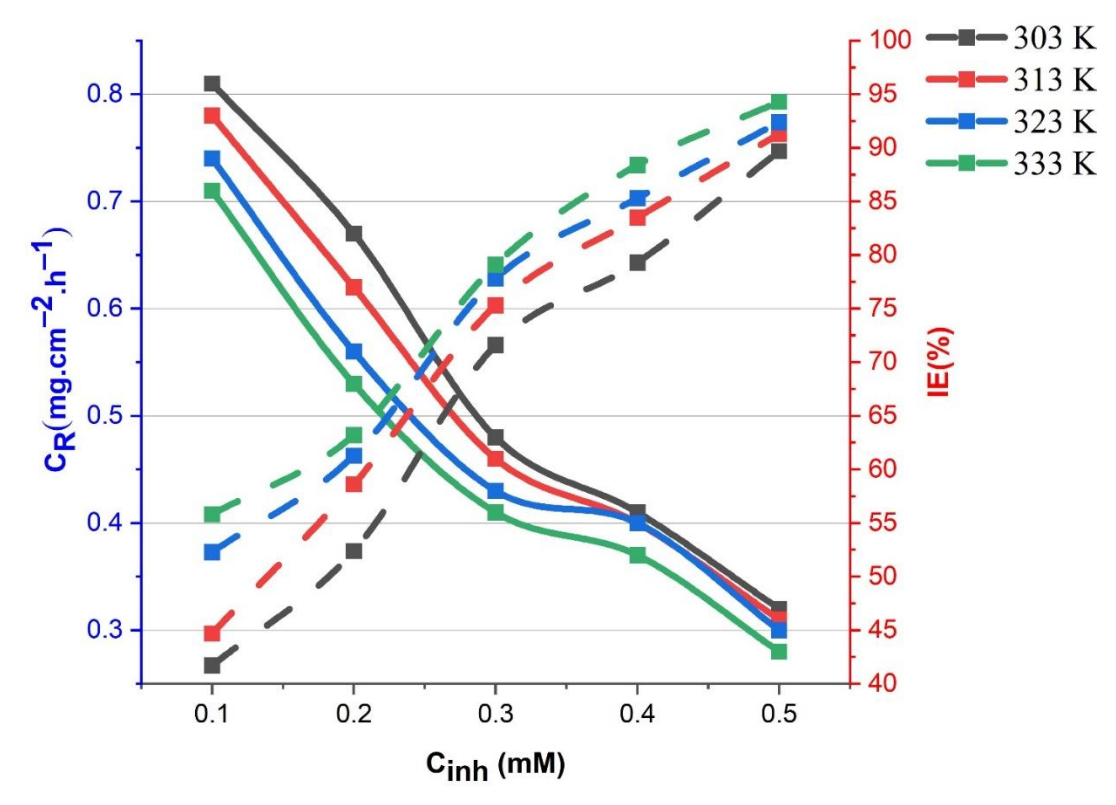


Figure 4. Effect of temperature and TMP concentration on C_R and inhibition efficiency (IE%) of carbon steel in 1 M HCl solution.

Higher TMP concentrations combined with elevated temperatures significantly enhance corrosion inhibition efficiency. At low concentrations (0.1–0.2 mM), *IE*% shows only moderate improvement due to limited surface coverage. In contrast, at 0.4–0.5 mM, TMP achieves near-complete coverage, maintaining *IE*% above 90% even at higher temperatures. This improved performance is attributed to increased molecular mobility, promoting stronger adsorption and formation of a dense, uniform protective layer that resists HCl attack [29]. The results are consistent with the Langmuir isotherm model, supporting monolayer adsorption. Overall, TMP proves to be a highly efficient inhibitor, especially under industrial conditions requiring both high temperature resistance and reliable surface protection.

3.2. Chemical stability of TMP

In our study, we studied carefully the chemical stability of TMP under the acidic conditions employed. This assessment consisted of a combination of visual inspections, spectral analyses, and periodic weight loss measurement over extended immersion time. The results exhibited that TMP remains chemically stable internally during the corrosion inhibition process. The structural characteristics of TMP corroborate its stability. As a Schiff base derivative, TMP has a thiazole ring bonded to a phenolic group, thereby establishing a stable conjugated system. This configuration, discussed in the literature for similar compounds [30], is said to provide resistance in acidic environments. Stability further supported by the

presence of hydroxyl (OH) in TMP: The hydroxyl group can intramolecularly hydrogen bond with the nitrogen atom of the thiazole ring, resulting in the formation of a six-membered ring. The formation of this type of intramolecular interaction imposes rigidity and stability to the molecular structure and hence reduces its tendency to undergo hydrolysis or decomposition in acidic environments. Overall, these findings and structural rationalizations establish that TMP maintains its function and efficacy as a corrosion inhibitor in acidic media, just as the stability was documented for similar Schiff base derivatives [31].

3.3. Adsorption isotherm

The adsorption phenomena signifying TMP on carbon steel were determined using Langmuir, Freundlich, and Temkin isotherm models. Among these, the most explanatory out of these three models is the Langmuir model, which has the best fitted to the experimental data as indicated by a high correlation coefficient (R^2 =0.978) and is associated with monolayer adsorption on a homogeneous adsorbent surface with very little or no intermolecular forces between the pollutant molecules adsorbed on the surface. This agrees with the signs from the tests that the inhibition efficiencies increased with concentration up to surface saturation; otherwise, higher correlation values of R^2 were found from the Freundlich and Temkin models compared to the Langmuir isotherm, thereby indicating multilayer adsorption and adsorbate-adsorbate interactions that are not significant in this system. Figure 5 represents a linear relationship, confirming the applicability of the Langmuir model to describe the adsorption process. The linearity of the plot indicates that TMP molecules form a monolayer on the carbon steel surface, with no significant interaction between adsorbed molecules. This suggests that the adsorption sites on the steel surface are uniform, and each TMP molecule adsorbs independently. The slope of the Langmuir plot, as shown in Figure 5, is 0.757, which is close to unity. This further validates the assumption of monolayer adsorption. The intercept (0.193) provides insight into the adsorption equilibrium constant (K_{ads}), as it is inversely proportional to K_{ads} [32]. A high K_{ads} value indicates strong adsorption of TMP molecules onto the steel surface, which enhances the corrosion inhibition efficiency. The adsorption of TMP molecules aligns with Langmuir isotherm assumptions, indicating that the process is spontaneous and energetically favorable. The consistent performance of TMP across a range of concentrations and temperatures (as shown in previous results) further supports this conclusion. The adsorption of TMP is the key mechanism behind its corrosion inhibition performance [34]. The Langmuir adsorption isotherm can be expressed mathematically as:

$$\frac{C_{\rm inh}}{\theta} = \frac{1}{K_{\rm ads}} + C_{\rm inh}$$

where, C_{inh} is the inhibitor concentration (mM), θ is the surface coverage of the inhibitor, and K_{ads} is the adsorption equilibrium constant.

Based on weight loss measurements, θ was calculated using the relation $\theta = (W_0 - W_i)/W_0$, where W_0 and W_i represent the weight loss in the absence and presence of the TMP, respectively. This approach assumes that the inhibitor predominantly functions *via* a blocking mechanism, where adsorbed molecules prevent direct contact between the metal surface and the corrosive environment. The adsorption behavior following the Langmuir isotherm supports the assumption of monolayer coverage and the direct correlation between inhibition efficiency and surface coverage [33].

From Figure 5, the intercept of the linear plot is 0.193, which is related to $K_{\rm ads}$ as follows:

$$K_{\text{ads}} = \frac{1}{\text{intercept}} = \frac{1}{0.193} = 5.18 \text{ mM}^{-1}$$

The standard Gibbs free energy of adsorption ($\Delta G_{\rm ads}^0$) is calculated using the following equation:

$$\Delta G_{\rm ads}^0 = -RT \ln(K_{\rm ads})$$

where: R is the universal gas constant (8.314 J·mol⁻¹·K⁻¹), T is the temperature in Kelvin (assume 303 K for this calculation), 55.5 is the molar concentration of water in the solution (mol·L⁻¹), K_{ads} is the adsorption equilibrium constant.

Substituting the values:

$$\Delta G_{\text{ads}}^0 = -8.314 \times 303 \ln(5.18) = -14.3 \text{ kJ/mol}$$

The value of $\Delta G_{\rm ads}^0$ provides insight into the adsorption mechanism. For $\Delta G_{\rm ads}^0$ values around $-20~{\rm kJ \cdot mol^{-1}}$ or more positive (e.g., $-10~{\rm kJ \cdot mol^{-1}}$), the mechanism is typically physisorption, which involves weak electrostatic interactions. For $\Delta G_{\rm ads}^0$ around $-40~{\rm kJ \cdot mol^{-1}}$ or more negative, the mechanism is **chemisorption**, which involves stronger chemical bonding between the inhibitor and the metal surface. The calculated $\Delta G_{\rm ads}^0 = -14.3~{\rm kJ \cdot mol^{-1}}$ suggests that the adsorption of TMP onto the carbon steel surface predominantly occurs through **physisorption** adsorption mechanism. This mechanism involves weak van der Waals interactions or hydrogen bonding, which align with the observed Langmuir adsorption behavior [35].

Even though the calculated $\Delta G_{\rm ads}^0 = -14.3 \, \rm kJ \cdot mol^{-1}$ suggests a physisorption mechanism, which is more plausible for the adsorption of TMP on the carbon steel surface. As shown in the temperature-dependent weight loss measurements (Figure 4), the inhibition efficiency of TMP increases with increasing temperature [36]. In contrast, purely physisorbed inhibitors often show decreased inhibition efficiency with rising temperature due to weaker physical interactions. The relatively high adsorption equilibrium constant indicates strong binding between TMP molecules and the steel surface. The Langmuir adsorption isotherm observed in Figure 5 confirms the formation of a monolayer of TMP on the steel surface. While this model accommodates physical adsorption mechanism, the

calculated $\Delta G_{\rm ads}^0 = -14.3~{\rm kJ\cdot mol^{-1}}$ falls within the range typically associated with physisorption. However, additional experimental evidence, such as increased inhibition efficiency with temperature, suggests that weak chemisorptive interactions may also be involved, leading to a mixed adsorption mechanism. Such intermediate $\Delta G_{\rm ads}^0$ values are often observed when physical interactions occur. TMP demonstrates high and stable inhibition efficiency even at extended immersion times and elevated temperatures, as shown in Figures 3 and 4. The adsorption of TMP on the carbon steel surface can be described as **physisorption**, involving initial weak interactions through van der Waals forces or hydrogen bonding, facilitating the adsorption of TMP molecules onto the steel surface. To further elucidate the nature of TMP adsorption on carbon steel, thermodynamic parameters such as enthalpy change (ΔH^0), entropy change (ΔS^0), and Gibbs free energy change (ΔG^0) were determined using Van't Hoff analysis. $K_{\rm ads}$ was measured at different temperatures (303 K–333 K), and the corresponding thermodynamic parameters were calculated. The relationship between $K_{\rm ads}$ and temperature is described by the Van't Hoff equation:

$$\ln K_{\text{ads}} = \frac{-\Delta H^0}{RT} + \frac{\Delta S^0}{R}$$

where, R is the universal gas constant (8.314 J·mol⁻¹·K⁻¹), T is the absolute temperature (K), ΔH^0 is the standard enthalpy change (kJ·mol⁻¹), and ΔS^0 is the standard entropy change (J·mol⁻¹·K⁻¹).

A Van't Hoff plot of $\ln K_{\rm ads}$ *versus* 1/T (Figure 6 and Table 1) was constructed, showing a good linear correlation (R^2 =0.99), indicating a consistent adsorption process.

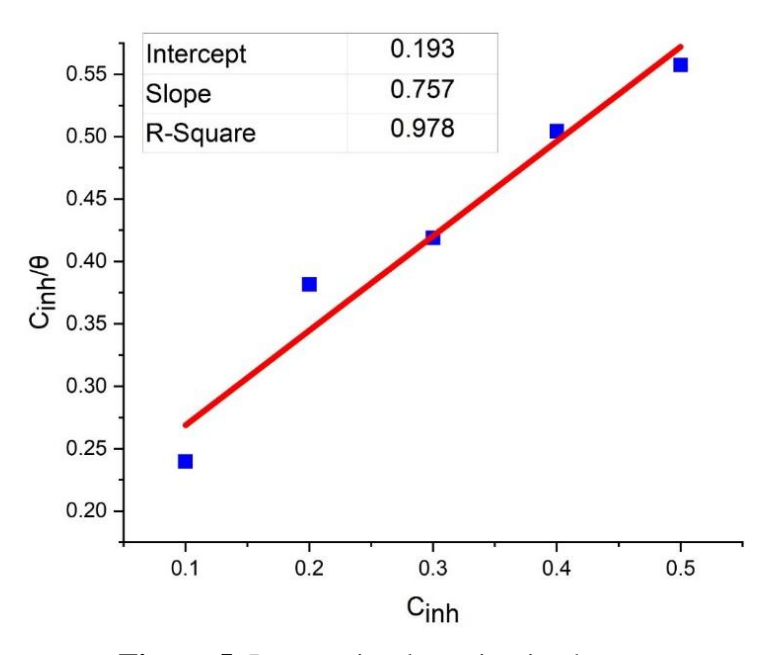


Figure 5. Langmuir adsorption isotherm.

Temp. (K)	$1/T (K^{-1})$	ln K _{ads}	$\Delta G_{ m ads}^{ m 0}$ (kJ·mol ⁻¹)
303	0.00330	1.6	-14.3
313	0.00319	1.9	-15.0
323	0.00310	2.1	-15.6
333	0.00300	2.4	-16.2

Table 1. Thermodynamic parameters for the adsorption of TMP on carbon steel at different temperatures.

From the slope of the Van't Hoff plot, the enthalpy and entropy changes were calculated and the **negative** ΔH^0 (-22.3 kJ·mol⁻¹) confirms that the adsorption of TMP onto the carbon steel surface is exothermic, meaning the process is favorable at lower temperatures and adsorption strength increases as temperature decreases, also the **negative** ΔS^0 (-25.4 J·mol⁻¹·K⁻¹) suggests a decrease in system randomness upon adsorption, indicating the formation of an organized monolayer on the metal surface. **Negative** $\Delta G_{\rm ads}^0$ **values** (-14.3 to -16.2 kJ·mol⁻¹) at different temperatures suggest that the adsorption is spontaneous and primarily driven by physisorption.

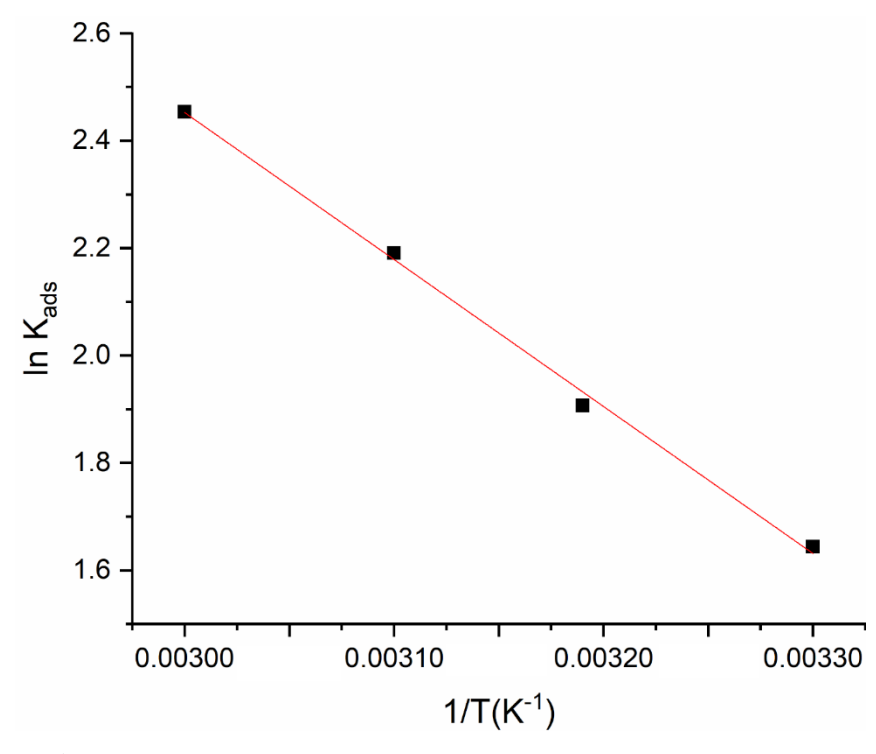


Figure 6. Van't Hoff plot for TMP adsorption on carbon steel.

3.4. DFT and its relation to corrosion inhibitors

The DFT results provide critical insights into the electronic properties of the TMP molecule and its ability to act as an effective corrosion inhibitor for carbon steel. The calculated parameters, such as the HOMO and LUMO energies, energy gap (ΔE), ionization potential

(I), electron affinity (A), electronegativity (γ), chemical hardness (η), chemical softness (σ), and electron transfer fraction (ΔN), are directly related to the inhibitor's reactivity and adsorption behavior. The HOMO energy (-9.458 eV) reflects the molecule's ability to donate electrons [37]. A higher HOMO energy (less negative) indicates a greater ability to donate electrons to the vacant d-orbitals of the metal surface. TMP's moderate HOMO energy suggests that it can effectively donate electrons through its lone pairs on nitrogen, oxygen, and sulfur atoms. The LUMO energy (-3.857 eV) represents the molecule's ability to accept electrons (Table 2). A lower LUMO energy indicates a greater ability to accept electrons from the metal surface, forming back-donation bonds. TMP's low LUMO energy suggests that it can accept electrons from the metal surface, stabilizing the adsorption process and enhancing the inhibitor's performance [24]. The energy gap ($\Delta E = 5.601 \text{ eV}$) between HOMO and LUMO indicates TMP's moderate reactivity – sufficient for adsorption while maintaining molecular stability. Its ionization potential (I=9.458 eV) and electron affinity (A = 3.857 eV) reflect its ability to donate and accept electrons, enabling strong donoracceptor interactions with the steel surface. TMP's high electronegativity ($\chi = 6.658 \text{ eV}$) promotes stable adsorption, while its moderate chemical hardness ($\eta = 2.801 \text{ eV}$) and softness ($\sigma = 0.357 \text{ eV}^{-1}$) support both reactivity and corrosion resistance. The positive electron transfer fraction (ΔN =0.061) confirms electron donation from TMP to the metal, reinforcing the inhibitor-metal bond. HOMO-LUMO interactions enable TMP to donate electrons via heteroatoms (N, O, S) and accept electrons from the steel, facilitating both interactions and back-donation. This dual interaction mechanism results in a stable, longlasting protective layer. Overall, DFT results confirm TMP's strong adsorption capability and effectiveness as a corrosion inhibitor in acidic media

Table 2. DFT Parameters and their values for TMP and their relevance to corrosion inhibition.

Parameter	Value	
Ionization potential (I) (eV)	9.458	
Electron affinity (A) (eV)	3.857	
HOMO energy (eV)	-9.458	
LUMO energy (eV)	-3.857	
Energy gap (eV)	5.601	
Electronegativity (χ) (eV)	6.6575	
Chemical hardness (η) (eV)	2.8005	
Chemical softness (σ) (eV ⁻¹)	0.357079	
Electron transfer fraction (ΔN)	0.06115	

The HOMO (Highest Occupied Molecular Orbital) of TMP contains electrons that can be donated to the metal's vacant *d*-orbitals. TMP's heteroatoms (N, O, and S) with lone pairs

act as primary donors (Figure 7). TMP's LUMO (Lowest Unoccupied Molecular Orbital) can accept electrons from the carbon steel surface through back-donation. This involves the flow of electrons from the filled orbitals of iron atoms into the LUMO of TMP, stabilizing the adsorption process. TMP's E_{HOMO} =-9.458 eV indicates a moderate electron-donating ability. Higher (less negative) HOMO energy typically enhances the donation of electrons, facilitating interactions on the metal surface. TMP's E_{LUMO} =-3.857 eV indicates its ability to accept electrons from the metal surface. Lower (more negative) LUMO energy allows better back-donation, complementing the electron-donating interaction. The calculated ΔN =0.061 confirms that TMP donates electrons to the carbon steel surface. A positive ΔN indicates that TMP acts as an electron donor, forming stable bonds with the metal. The electron transfer between TMP and the metal enables a back-donation of electrons from the metal to TMP's LUMO creates weak, reversible interactions. These interactions enhance the initial adsorption and surface coverage, improving the inhibitor's efficiency at low concentrations. TMP's molecular structure contains heteroatoms (N, O, and S) and conjugated systems, which play a vital role in electron transfer. Lone pairs on nitrogen atoms are highly available for donation to the metal surface, facilitating strong interactions. The hydroxyl group enhances electron donation and contributes to hydrogen bonding, which supports physisorption. Sulfur atoms in thiazole rings are soft bases, enhancing the interaction with the metal surface through both donation and back-donation. The electron transfer process directly affects TMP's inhibition performance in various way sch as, strong bond formation, surface coverage (Physisorption allows TMP molecules to spread uniformly on the steel surface, ensuring complete coverage and minimizing exposure to the corrosive environment), and stability of the protective film.

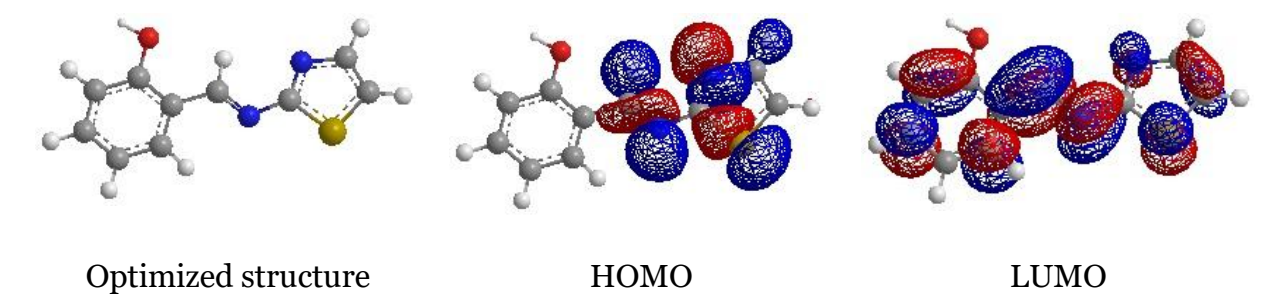


Figure 7. Optimized molecular structure, HOMO, and LUMO distribution of TMP based on DFT calculations.

3.5. Suggested inhibition mechanism

Figure 8 illustrates the proposed corrosion inhibition mechanism of TMP on carbon steel, emphasizing the dual interaction pathways of electron donation and back-donation during adsorption. TMP molecules adsorb onto the carbon steel surface, forming a protective layer that prevents the interaction of corrosive agents (HCl) with the metal [39–41]. The adsorption involves TMP molecules anchoring through functional groups (*e.g.*, nitrogen, oxygen, and sulfur atoms). The figure shows TMP molecules donating electrons (depicted as e⁻ arrows in

red) from their HOMO to the vacant d-orbitals of iron atoms on the steel surface. The steel surface also donates electrons (depicted as e⁺ arrows in green) from its orbitals to the LUMO of TMP molecules. This back-donation strengthens the inhibitor—metal interaction, further enhancing adsorption stability [42–44]. The combination of electron donation and back-donation creates a dense and stable monolayer of TMP on the steel surface. This barrier prevents the penetration of aggressive chloride ions and water molecules, effectively reducing corrosion rates. The Figure 7 supports the observation that the inhibition efficiency of TMP increases with temperature. The strong adsorption interaction ensures that TMP molecules remain effective across a range of concentrations, maintaining surface coverage and corrosion inhibition efficiency [45–47].

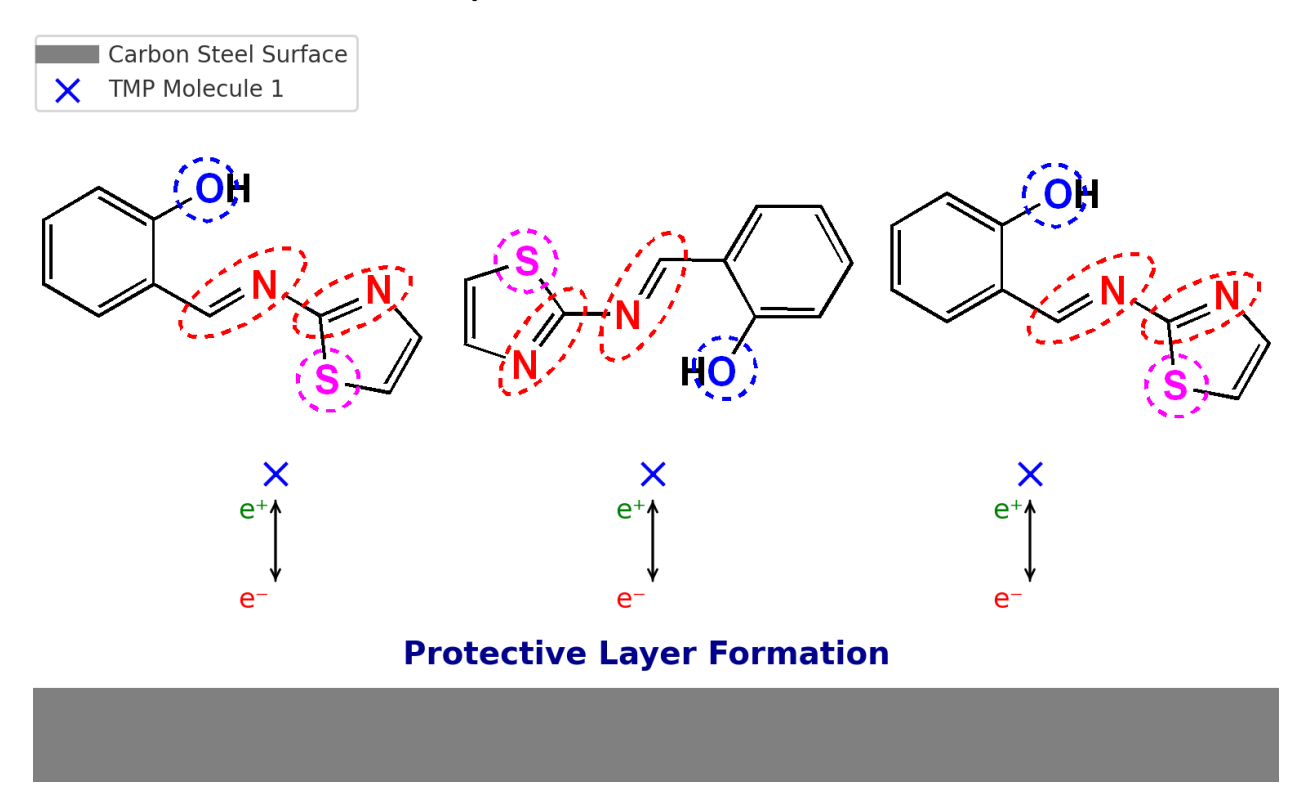


Figure 8. Suggested corrosion inhibition mechanism of TMP on carbon steel.

Conclusion

This research is focused on the corrosion inhibition behavior of TMP (2-((thiazol-2-ylimino)methyl)phenol) on carbon steel in 1 M HCl solution determined from weight loss measurements, adsorption isotherms and DFT calculations. It revealed complete elaboration of TMP as a corrosion inhibitor and its performance mechanisms. The major findings are as follows:

1. TMP presented evidently excellent corrosion inhibition; indeed, inhibition efficiencies were reached as high as 92.9% for a concentration of 0.5 mM at 303 K after 10 hours of immersion. The effectiveness increased with both the concentration of TMP and the time of immersion, proving that TMP could be an effective inhibitor.

- 2. The adsorption of TMP on the surface of carbon steel has confirmed the Langmuir adsorption isotherm, which proves the formation of a monolayer, stable monolayer, and thermodynamic parameters $\Delta G_{\rm ads}^0 = -14.3 \, \rm kJ \cdot mol^{-1}$ for Gibbs free energy of adsorption that favors physisorption adsorption.
- 3. DFT calculations represented most of the crucial electronic properties of TMP as HOMO energy $=-9.458 \,\text{eV}$, LUMO as $-3.857 \,\text{eV}$, having energy gap $= 5.601 \,\text{eV}$, which indicates TMP's ability to donate and accept electrons through its dual mechanism of electron transfer giving more stability for adsorption and for protection of the surface steel.
- 4. TMP promises to be a suitable candidate in the industrial application as the environment where carbon steel is subjected to acidic conditions such as in pickling and cleaning processes, is proving quite effective at *i.e.* high inhibition efficiency, temperature-dependent stability, organic structure environmentally friendly.

Funding Statement

Al-Ayen Iraqi University funded this research under the program titled, "Innovative Corrosion Inhibitors: A New Frontier in Materials Protection" (AUIQ-RFP2024-CI). The authors appreciate great effort for their financial support towards executing the research.

Acknowledgment

The authors hereby express their profound appreciation to Al-Ayen Iraqi University (AUIQ) for providing a grant for this study under the research project "Innovative Corrosion Inhibitors: A New Frontier in Materials Protection" (Project Code: AUIQ–RFP2024–CI). Their support and contribution towards this study was invaluable.

References

- 1. M. Errili, K. Tassaoui, A. Chraka, M. Damej, H. Rahal, N. Labjar, A. El Mahmoudi, K. Bougrin, A. Berisha and M. Benmessaoud, Synthesis and investigation of novel sulfonamide–1,2,3–triazoles corrosion inhibitors for E24 steel in 1 M HCl solution: a combination of modeling and experimental approaches, *Int. J. Corros. Scale Inhib.*, 2024, **13**, no. 3, 1607–1635. doi: 10.17675/2305-6894-2024-13-3-14
- 2. M.Y. El Sayed, A.M. Abdel-Gaber and H.T. Rahal, Safranin a potential corrosion inhibitor for mild steel in acidic media: a combined experimental and theoretical approach, *J. Failure Anal. Prev.*, 2019, **19**, 1174–1180. doi: 10.1007/s11668-019-00719-6
- 3. H.T. Rahal, A.M. Abdel-Gaber and G.O. Younes, Inhibition of steel corrosion in nitric acid by sulfur containing compounds, *Chem. Eng. Commun.*, 2016, **203**, no. 4, 435–445. doi: 10.1080/00986445.2015.1017636
- 4. H.T. Rahal, A.M. Abdel–Gaber and R. Awad, Corrosion behavior of a superconductor with different SnO₂ nanoparticles in simulated seawater solution, *Chem. Eng. Commun.*, 2017, **204**, no. 3, 348–355. doi: 10.1080/00986445.2016.1271794

- 5. E.B. Caldona, M. Zhang, G. Liang, T.K. Hollis, C.E. Webster, D.W. Smith Jr and D.O. Wipf, Corrosion inhibition of mild steel in acidic medium by simple azole-based aromatic compounds, *J. Electroanal. Chem.*, 2021, **880**, 114858. doi: 10.1016/j.jelechem.2020.114858
- 6. N. Benzbiria, A. Thoume, S. Echihi, M.E. Belghiti, A. Elmakssoudi, A. Zarrouk, M. Azzi and M. Zertoubi, Coupling of experimental and theoretical studies to apprehend the action of benzodiazepine derivative as a corrosion inhibitor of carbon steel in 1 M HCl, *J. Mol. Struct.*, 2023, **1281**, 13513. doi: 10.1016/j.molstruc.2023.135139
- 7. R.D. Salim, N. Betti, M. Hanoon and A.A. Al–Amiery, 2-(2,4-Dimethoxybenzylidene)-N-Phenylhydrazinecarbothioamide as an Efficient Corrosion Inhibitor for Mild Steel in Acidic Environment, Prog. Color, Color. Coat., 2021, 15, 45–52. doi: 10.30509/pccc.2021.166775.1105
- 8. E.S. Sherif, Corrosion and corrosion inhibition of aluminum in Arabian Gulf seawater and sodium chloride solutions by 3-amino-5-mercapto-1,2,4-triazole, *Int. J. Electrochem. Sci.*, 2011, **6**, no. 5, 1479–1492. doi: 10.1016/S1452-3981(23)15087-5
- 9. P.P. Venugopal, P.R. Kumari and D. Chakraborty, Anti-corrosion investigation of a new nitro veratraldehyde substituted imidazopyridine derivative Schiff base on mild steel surface in hydrochloric acid medium: Experimental, computational, surface morphological analysis, *Mater. Chem. Phys.*, 2022, **281**, 125855. doi: 10.1016/j.matchemphys.2022.125855
- 10. A. Altalhi, Anticorrosion investigation of new diazene-based Schiff base derivatives as safe corrosion inhibitors for API X65 steel pipelines in acidic oilfield formation water: synthesis, experimental, and computational studies, *ACS Omega*, 2023, **8**, no. 34, 31271–31280. doi: 10.1021/acsomega.3c03592
- 11. S.A. Abd El-Maksoud and H.H. Hassan, Electrochemical studies on the effect of (2E)-3-amino-2-phenylazo-but-2-enenitrile and its derivative on the behaviour of copper in nitric acid, *Mater. Corros.*, 2007, **58**, no. 5, 369–375. doi: 10.1002/maco.200604021
- 12. M. Ouakki, M. Galai and M. Cherkaoui, Imidazole derivatives as efficient and potential class of corrosion inhibitors for metals and alloys in aqueous electrolytes: A review, *J. Mol. Liq.*, 2022, **345**, 117815. doi: 10.1016/j.molliq.2021.117815
- 13. X. Sun, Y. Qiang, B. Hou, H. Zhu and H. Tian, Cabbage extract as an eco-friendly corrosion inhibitor for X70 steel in hydrochloric acid medium, *J. Mol. Liq.*, 2022, **362**, 119733. doi: 10.1016/j.molliq.2022.119733
- 14. M. Ghaderi, A.R. Saadatabadi, M. Mahdavian and S.A. Haddadi, pH-Sensitive polydopamine-La (III) complex decorated on carbon nanofiber toward on-demand release functioning of epoxy anti-corrosion coating, *Langmuir*, 2022, **38**, 11707–11723. doi: 10.1021/acs.langmuir.2c01801
- 15. B.S. Mahdi, M.K. Abbass, M.K. Mohsin, W.K. Al-Azzawi, M.M. Hanoon, M.H.H. AlKaabi, L.M. Shaker, A.A. Al-Amiery, W.N.R.W. Isahak, A.A.H. Kadhum and M.S. Takriff, Corrosion inhibition of mild steel in hydrochloric acid environment using terephthaldehyde based on Schiff base: Gravimetric, thermodynamic, and

- computational studies, *Molecules*, 2022, **27**, no. 15, 4857. doi: 10.3390/molecules27154857
- 16. M. Damej, M. Benmessaoud, S. Zehra, S. Kaya, H. Lgaz, A. Molhi, N. Labjar, S. El Hajjaji, A.A. Alrashdi and H.S. Lee, Experimental and theoretical explorations of S-alkylated mercaptobenzimidazole derivatives for use as corrosion inhibitors for carbon steel in HCl, *J. Mol. Liq.*, 2021, **331**, 115708. doi: 10.1016/j.molliq.2021.115708
- 17. A.M. Abdel-Gaber, H.T. Rahal and F.T. Beqai, *Eucalyptus* leaf extract as an ecofriendly corrosion inhibitor for mild steel in sulfuric and phosphoric acid solutions, *Int. J. Ind. Chem.*, 2020, **11**, 123–132. doi: 10.1007/s40090-020-00207-z
- 18. A.A. Al-Amiery, L.M. Shaker, A.A.H. Kadhum and M.S. Takriff, Synthesis, characterization and gravimetric studies of novel triazole-based compound, *Int. J. Low-Carbon Technol.*, 2020, **15**, no. 2, 164–170. doi: 10.1093/ijlct/ctz067
- 19. S.S. Al-Taweel, K.W.S. Al–Janabi, H.M. Luaibi, A.A. Al-Amiery and T.S. Gaaz, Evaluation and characterization of the symbiotic effect of benzylidene derivative with titanium dioxide nanoparticles on the inhibition of the chemical corrosion of mild steel *Int. J. Corros. Scale Inhib.*, 2019, **8**, no. 4, 1149–1169. doi: 10.17675/2305-6894-2019-8-4-21
- 20. S.B. Al-Baghdadi, A.A. Al-Amiery, T.S. Gaaz and A.H. Kadhum, Terephthalohydrazide and isophthalohydrazide as new corrosion inhibitors for mild steel in hydrochloric acid: Experimental and theoretical approaches, *Koroze Ochr. Mater.*, 2021, **65**, no. 1, 12–22. doi: 10.2478/kom-2021-0002
- 21. TM0169/G31-12a, Standard Guide for Laboratory Immersion Corrosion Testing of Metals, NACE International, Houston, TX, USA, 2012.
- 22. ASTM G 31-72, Standard Guide for Laboratory Immersion Corrosion Testing of Metals, American Society for Testing and Materials, Philadelphia, PA, USA, 1990.
- 23. M.E. Ansar, K. Tassaoui, A. Chraka, R. Hsissou, M. Damej, H.T. Rahal, S. El Hajjaji and M. Benmessaoud, Electrochemical, thermodynamic, and theoretical study of the corrosion inhibition properties of triglycidyloxy tripropylamine triazine on E24 steel in 1 M HCl, *Int. J. Corros. Scale Inhib.*, 2024, **13**, no. 4, 2607–2637. doi: 10.17675/2305-6894-2024-13-4-38
- 24. M. Hrimla, L. Bahsis, M.R. Laamari, M. Julve and S.E. Stiriba, An overview on the performance of 1,2,3-triazole derivatives as corrosion inhibitors for metal surfaces, *Int. J. Mol. Sci.*, 2021, **23**, no. 1, 16. doi: 10.3390/ijms23010016
- 25. N.S. Abdelshafi, A.A. Farag, F.E.T. Heakal, A.S. Badran, K.M. Abdel-Azim, A.R. Manar El Sayed and M.A. Ibrahim, In-depth experimental assessment of two new aminocoumarin derivatives as corrosion inhibitors for carbon steel in HCl media combined with AFM, SEM/EDX, contact angle, and DFT/MDS simulations, *J. Mol. Struct.*, 2024, 1304, 137638. doi: 10.1016/j.molstruc.2024.137638
- 26. Yu.I. Kuznetsov, Triazoles as a class of multifunctional corrosion inhibitors. A review. Part I. 1,2,3-Benzotriazole and its derivatives. Copper, zinc and their alloys, *Int. J. Corros. Scale Inhib.*, 2018, **7**, no. 3, 271–307. doi: 10.17675/2305-6894-2018-7-3-1

- 27. M. Bairy, M. Pais, P.P. Kumari and S.A. Rao, Hydrazinecarbothioamide Derivative as an Effective Inhibitor for Corrosion Control: Electrochemical, Surface and Theoretical Studies, *J. Bio Tribo Corros.*, 2022, **8**, no. 5, 1–15. doi: 10.1007/s40735-021-00604-6
- 28. V.K. Shenoy, P.P. Venugopal, R.P.D. Kumari and D. Chakraborty, Anti-corrosion investigation of a new nitro veratraldehyde substituted imidazopyridine derivative Schiff base on mild steel surface in hydrochloric acid medium: Experimental, computational, surface morphological analysis, *Mater. Chem. Phys.*, 2022, **281**, 125855. doi: 10.1016/j.matchemphys.2022.125855
- 29. R. Touir, N. Errahmany, M. Rbaa, F. Benhiba, M. Doubi, E.H. EL Kafssaoui and B. Lakhrissi, Experimental and computational chemistry investigation of the molecular structures of new synthetic quinazolinone derivatives as acid corrosion inhibitors for mild steel, *J. Mol. Struct.*, 2024, **1303**, 137499. doi: 10.1016/j.molstruc.2024.137499
- 30. M. Galai, K. Dahmani, O. Kharbouch, M. Rbaa, N. Alzeqri, L. Guo, A.A. AlObaid, A. Hmada, N. Dkhireche, E. Ech-chihbi, M. Ouakki, M. Ebn Touhami and I. Warad, Surface analysis and interface properties of a newly synthesized quinoline-derivative corrosion inhibitor for mild steel in acid pickling bath: Mechanistic exploration through electrochemical, XPS, AFM, contact angle, SEM/EDS, and computational studies, *J. Phys. Chem. Solids*, 2024, **184**, 11169. doi: 10.1016/j.jpcs.2023.111681
- 31. H. Zhang, Z. Yang, L. Zhang, W. Yue, Y. Zhu and X. Zhang, Inhibition performance of halogen-substituted benzaldehyde thiosemicarbazones as corrosion inhibitors for mild steel in hydrochloric acid solution, *RSC Adv.*, 2022, **12**, 30611–30625. doi: 10.1039/D2RA05690A
- 32. Yu.I. Kuznetsov, N.N. Andreev and S.S. Vesely, Why we reject papers with calculations of inhibitor adsorption based on data on protective effects, *Int. J. Corros. Scale Inhib.*, 2015, **4**, no. 2, 108–109.
- 33. E.E. El-Katori, R.A. El-Saeed and M.M. Abdou, Anti-corrosion and anti-microbial evaluation of novel water-soluble bis azo pyrazole derivative for carbon steel pipelines in petroleum industries by experimental and theoretical studies, *Arabian J. Chem.*, 2022, **15**, no. 12, 104373. doi: 10.1016/j.arabjc.2022.104373
- 34. H.M.A. El-Lateef, M.M. Khalaf, K. Shalabi and A.A. Abdelhamid, Efficient Synthesis of 6,7-Dihydro-5H-cyclopenta[b]pyridine-3-carbonitrile Compounds and Their Applicability As Inhibitor Films for Steel Alloy Corrosion: Collective Computational and Practical Approaches, *ACS Omega*, 2022, **7**, no. 28, 24727–24745. doi: 10.1021/acsomega.2c02639
- 35. M.A. Hegazy, M. Abdallah, M.K. Awad and M. Rezk, Three novel di-quaternary ammonium salts as corrosion inhibitors for API X65 steel pipeline in acidic solution. Part I: Experimental results, *Corros. Sci.*, 2014, **81**, 54–64. doi: 10.1016/j.corsci.2013.12.010

- 36. P.T. Scaria, P. Shetty, P. Preethi and S. Kagatikar, 2-Aminobenzothiazole as an efficient corrosion inhibitor of AA6061-T6 in 0.5 M HCl medium: electrochemical, surface morphological, and theoretical study, *J. Appl. Electrochem.*, 2022, **52**, no. 11, 1–15. doi: 10.1007/s10800-022-01742-6
- 37. R. Yıldız, An electrochemical and theoretical evaluation of 4,6-diamino-2-pyrimidinethiol as a corrosion inhibitor for mild steel in HCl solutions, *Corros. Sci.*, 2015, **90**, 544–553. doi: 10.1016/j.corsci.2014.10.047
- 38. X. Li, S. Deng and X. Xie, Experimental and theoretical study on corrosion inhibition of oxime compounds for aluminium in HCl solution, *Corros. Sci.*, 2014, **81**, 162–175. doi: 10.1016/j.corsci.2013.12.021
- 39. C. Verma, M.A. Quraishi and K.Y. Rhee, Corrosion inhibition relevance of semicarbazides: electronic structure, reactivity and coordination chemistry, *Rev. Chem. Eng.*, 2022, **39**, no. 6, 1005–1026. doi: 10.1515/revce-2022-0009
- 40. K.M. Shainy, A.R. Prasad, A. Thomas and A. Joseph, Synergistic interaction of 2-amino 4-methyl benzothiazole (AMBT) and benzotriazole (BTZ) offers excellent protection to mild steel exposed in acid atmosphere at elevated temperatures: Electrochemical, computational and surface studies, *Egypt. J. Pet.*, 2019, **28**, no. 1, 35–45. doi: 10.1016/j.ejpe.2018.10.002
- 41. I.A. Alkadir Aziz, I.A. Annon, M.H. Abdulkareem, M.M. Hanoon, M.H. Alkaabi, L.M. Shaker, A.A. Alamiery, W.N. Wan Isahak and M.S. Takriff, Insights into corrosion inhibition behavior of a 5-mercapto-1,2,4-triazole derivative for mild steel in hydrochloric acid solution: Experimental and DFT studies, *Lubricants*, 2021, **9**, no. 12, 122. doi: 10.3390/lubricants9120122
- 42. M. Rehioui, F. Lazrak, S. Lahmidi, S. Benmekki, W.S. El-Yazeed, H. Erramli and N. Hajjaji, 1,2,4-triazole-5-thione derivative for inhibiting carbon steel corrosion in 1 M HCl: Synthesis, electrochemical, SEM/EDX, DFT, and MD investigations, *J. Mol. Struct.*, 2024, 1303, 137577. doi: 10.1016/j.molstruc.2024.137577
- 43. E.S. Sherif, Corrosion and corrosion inhibition of aluminum in Arabian Gulf seawater and sodium chloride solutions by 3-amino-5-mercapto-1,2,4-triazole, *Int. J. Electrochem. Sci.*, 2011, **6**, no. 5, 1479–1492. doi: 10.1016/S1452-3981(23)15087-5
- 44. S.A. Abd El-Maksoud and H.H. Hassan, Electrochemical studies on the effect of (2E)-3-amino-2-phenylazo-but-2-enenitrile and its derivative on the behaviour of copper in nitric acid, *Mater. Corros.*, 2007, **58**, no. 5, 369–375. doi: 10.1002/maco.200604021
- 45. M. Hrimla, L. Bahsis, M.R. Laamari, M. Julve and S.E. Stiriba, An overview on the performance of 1,2,3-triazole derivatives as corrosion inhibitors for metal surfaces, *Int. J. Mol. Sci.*, 2021, **23**, no. 1, 16. doi: 10.3390/ijms23010016
- 46. A. Kadhim, N. Betti, H.A. Al-Bahrani, M.K.S. Al-Ghezi, T. Gaaz, A.H. Kadhum and A. Alamiery, A mini review on corrosion, inhibitors and mechanism types of mild steel inhibition in an acidic environment, *Int. J. Corros. Scale Inhib.*, 2021, **10**, no. 3, 861–884. doi: 10.17675/2305-6894-2021-10-3-2

47. E. Koh and S. Park, Self-anticorrosion performance efficiency of renewable dimer-acid-based polyol microcapsules containing corrosion inhibitors with two triazole groups, *Prog. Org. Coat.*, 2017, **109**, 61–69. doi: 10.1016/j.porgcoat.2017.04.021

